Journal of Materials Science and Engineering B 14 (1-3) (2024) 7-13
doi: 10.17265/2161-6221/2024.1-3.002

First-Principles Study of the New Layered Ternary Metal Telluride, Eu_2InTe_5

Yiming Yu, Yuchen Zou, Jianan Bian and Li Zhang
School of Science, Jiliang University, Hangzhou 310018, China

Abstract: In this study, we performed first-principles calculations using the VASP (Vienna Ab initio Simulation) software package to investigate the crystal structure, electronic structure, and optical properties of a new layered ternary metal chalcogenide, Eu_2InTe_5. Our results show that Eu_2InTe_5 is a non-zero-gap metal with a layered structure characterized by strong intra-layer atomic bonding and weak inter-layer interaction, which suggests its potential application as a nanomaterial. We also studied the optical properties, including the absorption coefficient, imaginary and real parts of the complex dielectric constant, and found that Eu_2InTe_5 exhibits strong photoresponse characteristics at the junction of ultraviolet and visible light as well as blue-green light, with peaks at wavelengths of 389 nm and 477 nm. This suggests that it could be used in the development of UV (ultraviolet) detectors and other optoelectronic devices. Furthermore, due to its strong absorption, low loss, and low reflectivity, Eu_2InTe_5 has the potential to be used as a promising photovoltaic absorption layer in solar cells.

Key words: Ternary metal telluride, first-principles calculations, layered structure, optical properties.

1. Introduction

In recent years, the layered structure of graphene [1] has opened up new prospects for exploring the properties of other 2D (two-dimensional) layered crystals. Layered materials have two obvious advantages: a larger specific surface area and a smaller atomic layer thickness. The former can promote the generation of more photon absorption in materials, while the latter can significantly improve the transmission rate of carriers in materials [2-4]. However, due to the zero-bandgap nature of graphene and its high cost, it is difficult to commercialize. Therefore, exploring more layered materials has significant implications for various fields, including physics, chemistry, materials science, and engineering.

Among these layered crystals, 2D metal chalcogenides have been widely explored due to their intriguing physical phenomena [5, 6]. As one of its important constituents [7-9], metal tellurides require higher external energy or surface-active agents to enhance their reactivity, making their preparation more difficult compared to their sulfur and selenium counterparts. Additionally, telluride research started later due to their low activity. However, some scholars have discovered telluride materials with superior properties, such as CdTe, ZnTe, and PbTe. CdTe has a high absorption coefficient for solar light, and its bandgap is approximately 1.45 eV. It has two types of conductivity, n-type and p-type, and both carrier mobilities are high. It can exhibit the quantum confinement effect of emission characteristics with size change at room temperature, and its emission range includes the entire visible light region and near-infrared region, which can be used for infrared detection, optoelectronic modulators, and bio-labeling. ZnTe is also a good optoelectronic material that can be used to make green light-emitting diodes. Additionally, PbTe has significant optoelectronic conductivity properties and has achieved important results in the field of solar cells.

A recent article on the preparation and physical

Corresponding author: Yiming Yu, postgraduate, research fields: condensed matter physics.

properties of ternary europium telluride compound Eu_2InTe_5 has been reported [10]. Based on this, the present study investigates the compound Eu_2InTe_5 by first-principles calculations of its crystal structure, electrical and optical properties, and reveals the various physical properties of its layered metal telluride structure. This study fills the gap in the current theoretical research on layered ternary europium telluride compounds, improves its computational system, and provides a better theoretical basis for future related calculations and experiments, which is beneficial for the development of Eu-Te family compounds in future application areas.

2. Calculation Method

In this paper, the calculations of crystal structures and electronic and optical properties were performed using DFT (density functional theory) implemented in the VASP (Vienna Ab initio Simulation) Package [11]. The GGA (generalized gradient approximation) was employed using the exchange and correlation function of PBE (Perdew, Burke, and Ernzerhof) [12]. The Monkhorst Pack [13] *k*-point grid of 4 × 4 × 4 is adopted, and the plane wave cutoff energy of 400 eV and the energy convergence of 10^{-6} eV are used to optimize the structure. Electronic and optical properties were calculated using PBE with a cutoff energy of 400 eV.

3. Results and Discussion

3.1 Crystal Structure

Fig. 1 shows the optimized crystal structure of Eu_2InTe_5, with space group IMM2 (No. 44) and lattice constants $a = b = c = 8.66$ Å. The unit cell of Eu_2InTe_5 consists of $[EuTe_2]^{2+}$, $[InTe_2]^-$, and $[Te_2]^-$, with $[EuTe_2]^{2+}$ located at the four corners of the unit cell and $[InTe_2]^-$ and $[Te_2]^-$ distributed inside the unit cell, exhibiting a layered structure.

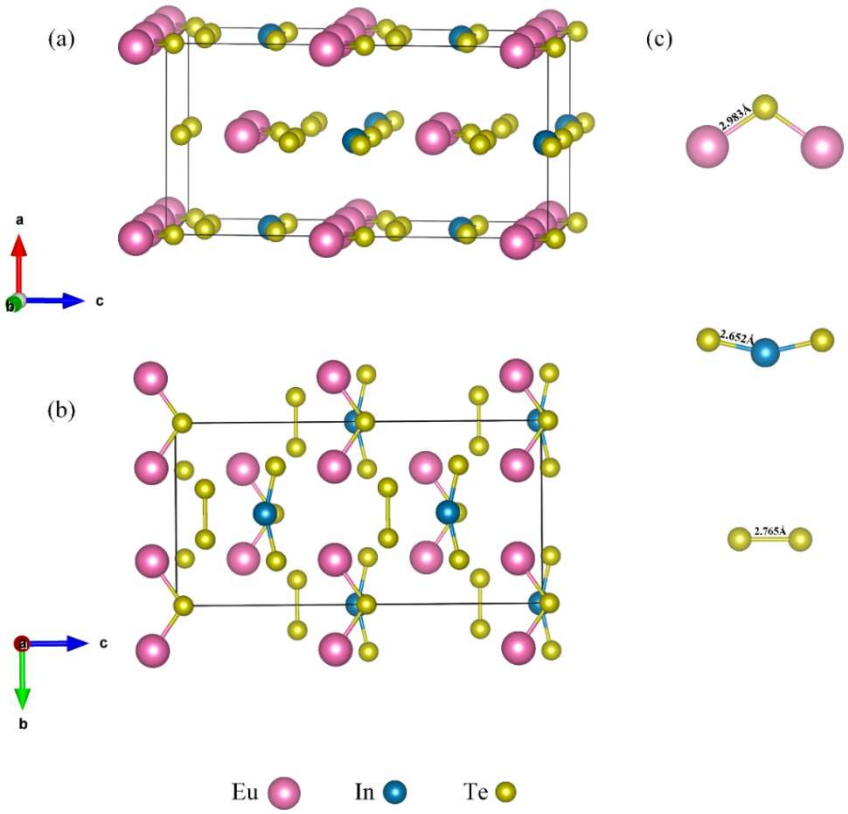

Fig. 1 (a) The front view along the b axis; (b) The top view along the a axis; (c) The Eu-Te bond, In-Te bond, Te-Te bond and their bond lengths.

As shown in Fig. 1a, in order to better observe the layered distribution characteristics of the crystal structure of Eu_2InTe_5, we extended the unit cell along the c-axis direction (pink represents Eu atoms, blue represents In atoms, and yellow represents Te atoms). The layered structure of Eu_2InTe_5 can be clearly seen, and the layers are arranged staggeredly. The interlayer spacing is measured to be 5 Å. Fig. 1b shows a top view from above the a-axis, where each layer is composed of $[EuTe_2]^{2+}$, $[InTe_2]^-$, and $[Te_2]^-$ ions formed by tightly bound Eu-Te, In-Te, and Te-Te bonds. The Eu-Te bond length is about 2.98 Å, the In-Te bond length is about 2.65 Å, indicating strong interaction forces between them. The Te-Te bond length is about 2.77 Å, which is close to the covalent 2.80 Å of an ordinary Te-Te bond.

From the perspective of material structure, the atomic distances between atoms in the same layer of Eu_2InTe_5 are closer and the binding is stronger, while the distances between atoms in adjacent layers are farther and the binding force is weaker. Therefore, if Eu_2InTe_5 material is subjected to a certain external force, it may cause the bonding between atoms in different layers to be broken, leading to the separation of single-layer Eu_2InTe_5, which may be prepared as a nano-scale material. Based on this property, other layers may be inserted between layers for doping experiments. In addition, the formation energy of Eu_2InTe_5 was calculated to be -3.02 J, indicating its good stability and ability to exist in nature.

3.2 Electronic Structure

In addition to crystal structure, electronic structure is also a key indicator of materials properties. In this paper, all DOS (density of states) and band structures are drawn at zero Fermi level. Fig. 2a shows the band structure of Eu_2InTe_5, where the Fermi level is shifted towards the valence band edge. This is because Te atoms can connect to form polymeric anions Te_n^{2-} (n = 2~6), which carry a negative two charge. However, in Eu_2InTe_5 calculated in this study, the Te anion group is $[Te_2]^-$, which has one less valence electron and induces holes in the structure, causing the Fermi level to shift [14]. Nevertheless, this does not affect our measurement of the band gap. The conduction band minimum and valence band maximum both occur at the high symmetry point G in the Brillouin zone, and we measure a direct band gap of 0.67 eV for Eu_2InTe_5. Compared to zero band gap metals, Eu_2InTe_5 metal compounds with finite band gaps are more controllable and may yield more excellent properties through further doping experiments, making this material a more versatile option for future applications.

The TDOS (total density of states) and PDOS (partial density of states) of Eu_2InTe_5 are shown in Figs. 2c and 2d. The valence band maximum energy from -2.0 eV to 0 eV is mainly contributed by Eu-4d and Te-5p orbitals, forming Eu-Te bonds around the Fermi level. Therefore, the Eu-Te bonds within each layer mainly determine the electronic structure near the band gap, while the conduction band is mainly composed of Te-5p orbitals. It can be inferred that In almost has no effect on the energy bands near the Fermi level.

In order to better explore the contributions of Eu_2InTe_5 elements to the electronic structure, the contributions of different orbitals of each element are also important in addition to the orbitals near the Fermi level (Fig. 2d). Eu-5p, In-5s, and In-4d occupy energy levels of -18 eV, -4 eV, and -10 eV, respectively, while Te-5s contributes at -11 to -8 eV. Thus, it can be seen that In only has a contribution at high energy levels, while its contribution near the Fermi level is minimal.

Table 1 presents the Bader charge differences for each element in Eu_2InTe_5. By combining the results with Fig. 2b, it is observed that Eu and In form Eu-Te and In-Te bonds, constituting $[EuTe_2]^{2+}$ and $[InTe_2]^-$ ions, respectively. Both Eu and In lose electrons to form positively charged ions, while Te forms negatively charged ions.

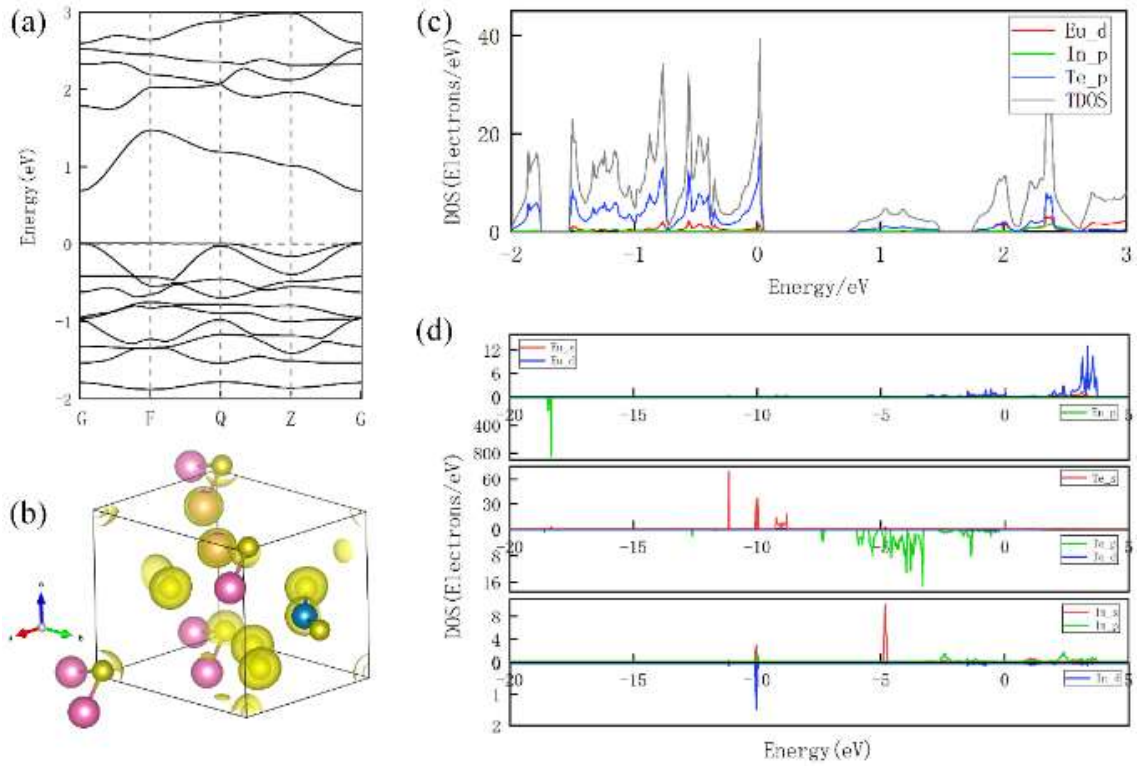

Fig. 2 (a) The band structure; (b) The charge distribution diagramband; (c) The TDOS; (d) The PDOS.

Table 1 Charge states of Eu_2InTe_5 compounds based on Bader charge analysis.

Eu_2InTe_5	Bader charge state	The average value
Eu	+1.86	+1.63
Eu	+1.39	
In	+0.65	+0.65
Te	-0.46	
Te	-0.44	
Te	-1.12	-0.68
Te	-0.69	
Te	-0.69	

3.3 Optical Structure

In addition to using band theory to explain the properties of Eu_2InTe_5, optical properties are also an important indicator of material characteristics. We calculated the real and imaginary parts of the dielectric function of Eu_2InTe_5 using a formula and plotted the optical absorption coefficient spectrum to study the optical properties of Eu_2InTe_5.

$$\varepsilon(\omega) = \varepsilon_1(\omega) + i\varepsilon_2(\omega) \quad (1)$$

$$\alpha(\omega) = \frac{\sqrt{2}e}{\hbar c}\left[(\varepsilon_1^2 + \varepsilon_2^2)^{1/2} - \varepsilon_1\right]^{1/2} \quad (2)$$

In Eq. (1), ε is the complex dielectric constant, and $\mathrm{Re}(\varepsilon_1)$ and $\mathrm{Im}(\varepsilon_2)$ are the real and imaginary parts of the complex dielectric coefficient, respectively. Eq. (2) represents the absorption coefficient $\alpha(\omega)$ [15].

Figs. 3a and 3b respectively show the relationship between the absorption coefficient and energy, and between the absorption coefficient and wavelength. By combining the two figures, it can be observed that Eu_2InTe_5 has two peaks, with the highest peak at a wavelength of 389 nm (energy of 3.18 eV) and the secondary peak at a wavelength of 477 nm (energy of 2.59 eV). This indicates that Eu_2InTe_5 has strong light absorption at the boundary of ultraviolet and visible light as well as at the boundary of blue-green light, and its high response to ultraviolet radiation makes it a promising material for the preparation of ultraviolet-blind detectors. Compared with other common metal compounds, Eu_2InTe_5 can absorb a wider range of visible light waves, exhibiting significant and

anomalous optical responses in the broad-band range from visible to far-infrared light.

Figs. 3c and 3d show the $Re(\varepsilon_1)$ and the $Im(\varepsilon_2)$ of the dielectric function of Eu_2InTe_5. The $Re(\varepsilon_1)$ typically describes the degree of polarization of the medium under an external electric field, which can be obtained through the Kramers-Kronig relation [16]. The $Im(\varepsilon_2)$ describes the transition of electrons from occupied states to unoccupied states when light passes through the medium and can be obtained through the momentum matrix of electronic transitions [17, 18]. From the figure, it can be observed that the dielectric function fluctuates in the lower energy region, and the real part of the dielectric function exhibits a peak at 2.09 eV, while the imaginary part exhibits a peak at 3.18 eV. This main peak, located within the visible light range, is formed by electron transitions from the top valence band to the bottom conduction band. At energies above 20 eV, the real part tends to zero, while the imaginary part tends to zero above 10 eV.

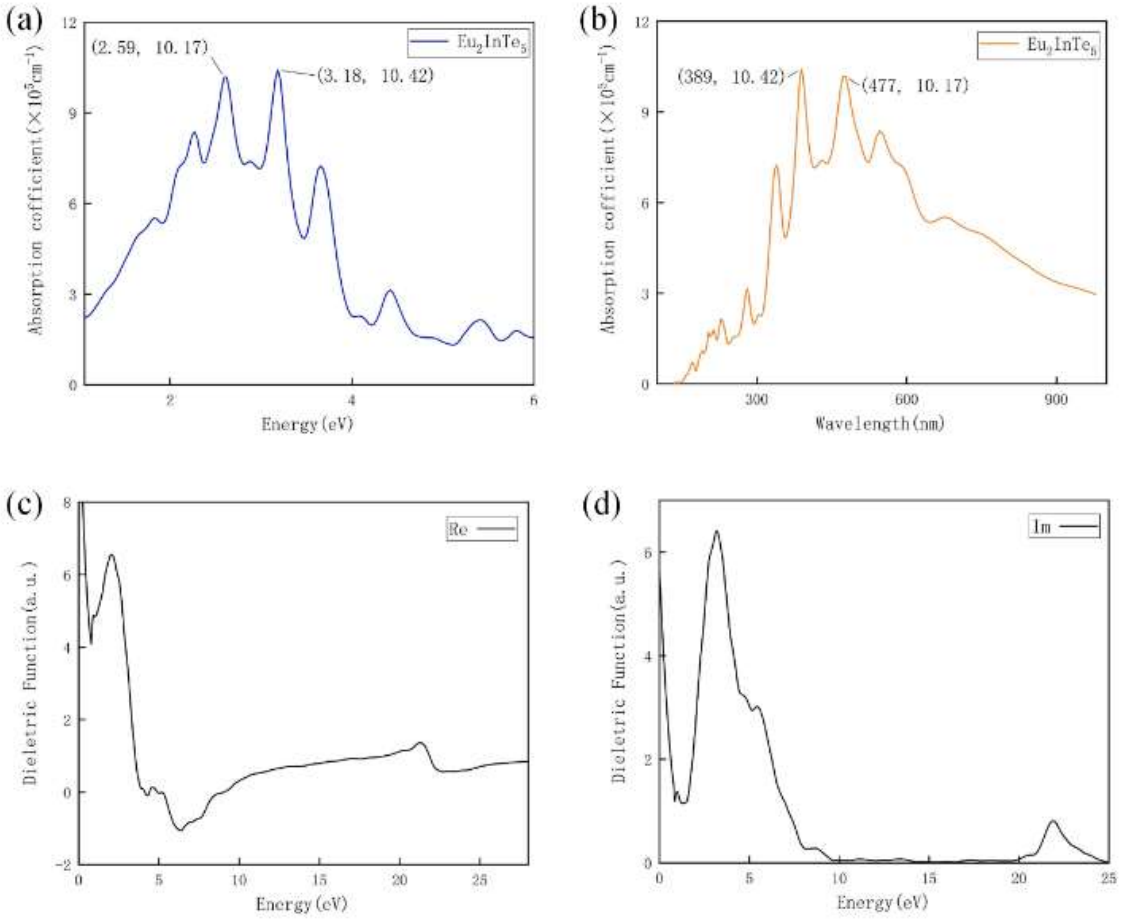

Fig. 3 (a) The relationship between optical absorption and energy; (b) The relationship between optical absorption and wavelength; (c) The real part of dielectric function; (d) The imaginary part of the dielectric function.

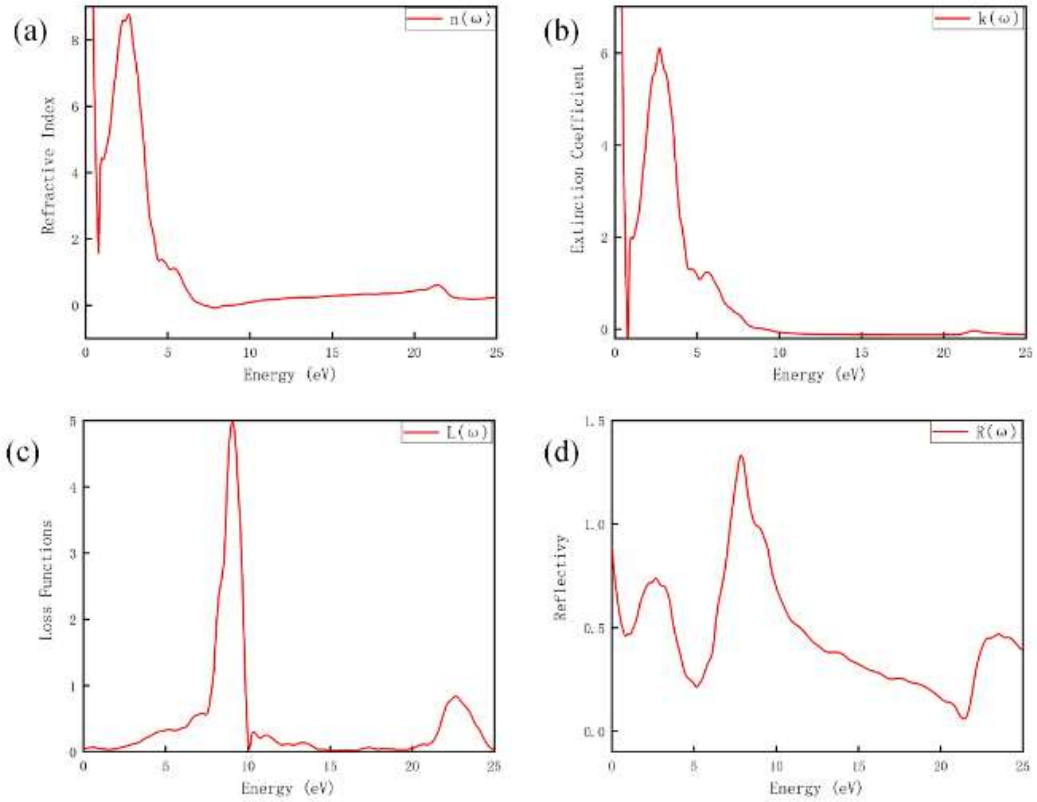

Fig. 4 (a) The refractive index n(ω); (b) The extinction coefficient k(ω); (c) The absorption coefficient L(ω); (d) The reflectance R(ω).

The complex refractive index of a solid can be expressed as $\tilde{n}(\omega) = n(\omega) + ik(\omega)$. In Figs. 4a and 4b, we can observe that the $n(\omega)$and $k(\omega)$ exhibit similar trends to the $Re(\varepsilon_1)$ and the $Im(\varepsilon_2)$ of the dielectric function in Figs. 3c and 3d. From Fig. 4a, it can be seen that the refractive index of Eu_2InTe_5 sharply decreases in the infrared region but reaches a maximum value of 8.77 at an incident photon energy of 2.62 eV in the visible range before rapidly decreasing and reaching a minimum value within the energy range of 7.1-8.9 eV. Subsequently, it gradually levels off and approaches zero at high energies.

The loss function of Eu_2InTe_5 describes the attenuation of light passing through a homogeneous medium, as shown in Fig. 4c. Its maximum value in the visible range is 0.13, indicating that Eu_2InTe_5 has very low losses in this region. However, it exhibits extremely high losses within the energy range of 7.5-10.1 eV in the ultraviolet region. Fig. 4d displays the reflectance of Eu_2InTe_5. The calculated static reflectivity coefficient R(0) is 0.89, and its value is very small in the observed energy range, reaching maximum values of approximately 0.74 and 1.33 in the visible and ultraviolet regions, respectively. We should point out that the peak of the loss function corresponds to the inflection point of the reflectance.

4. Conclusions

We performed first-principles calculations using the VASP software based on DFT with the GGA to study the crystal structure, electronic structure, and optical properties of Eu_2InTe_5. Our results showed that Eu_2InTe_5 is a non-zero bandgap metal with a direct bandgap of 0.67 eV, and the valence band maximum is mainly contributed by Eu-4d and Te-5p orbitals, forming the Eu-Te bond and determining the electronic structure near the bandgap. On the other hand, the conduction band is mainly composed of Te-5p orbitals,

indicating that the In element has little effect on the bands near the Fermi level. Furthermore, the Bader charge analysis further confirms the ionic bonds in the layered structure. In terms of optical properties, Eu_2InTe_5 exhibits strong light absorption at the boundary between UV and visible light, and has high refractive index, high reflectivity, and low loss in the visible range. These properties make it not only suitable for the fabrication of UV detectors but also ideal for various optoelectronic devices in the visible range. In future work, we will further deepen our understanding of the layered structure and optical properties, and achieve a better consistency between theoretical calculations and experimental data.

References

[1] Novoselov, K. S., Geim, A. K., Morozov, S. V., Jiang, D., Zhang, Y., Dubonos, S. V., Grigorieva, I. V., and Firsov, A. A. 2004. "Electric Field Effect in Atomically Thin Carbon Films." *Science* 306: 666-9.

[2] Chhowalla, M., Jena, D., & Zhang, H. 2016. "Two-Dimensional Semiconductors for Transistors." *Nature Reviews Materials* 1 (11): 1-15.

[3] Wang, J., Hernandez, Y., Lotya, M., Coleman, J. N., and Blau, W. J. 2009. "Broadband Nonlinear Optical Response of Graphene Dispersions." *Advanced Materials* 21 (23): 2430-5.

[4] Zhou, J., Lin, J., Huang, X., Zhou, Y., Chen, Y., Xia, J., et al. 2018. "A Library of Atomically Thin Metal Chalcogenides." *Nature* 556: 355-9.

[5] Wang, H., Li, C., Fang, P., Zhang, Z., and Zhang, J. Z. 2018. "Synthesis, Properties, and Optoelectronic Applications of Two-Dimensional MoS2 and MoS2-Based Heterostructures." *Chem. Soc. Rev*. 47: 6101-27.

[6] Zhou, J., Lin, J., Huang, X., Zhou, Y., Chen, Y., Xia, J., Wang, H., Xie, Y., Yu, H., and Lei, J. 2018. "A Library of Atomically Thin Metal Chalcogenides." *Nature* 556: 355-9.

[7] Zhang, F., Zhang, H., Krylyuk, S., Milligan, C. A., Zhu, Y., Zemlyanov, D. Y., et al. 2019. "Electric-Field Induced Structural Transition in Vertical $MoTe_2$ and $Mo_{1-x}W_xTe_2$ Based Resistive Memories." *Nature Materials* 18 (1): 55-61.

[8] Li, Y., Duerloo, K. A. N., Wauson, K., and Reed, E. J. 2016. "Structural Semiconductor-to-Semimetal Phase Transition in Two-Dimensional Materials Induced by Electrostatic Gating." *Nature Communications* 7: 1-8.

[9] Su, J., Liu, K., Wang, F., Jin, B., Guo, Y., Liu, G., Li, H., and Zhai, T. 2019. "Van der Waals 2D Transition Metal Tellurides." *Advanced Materials Interfaces* 6 (19): 1-17.

[10] Zheng, X., Boubeche, M., Wang, W., Fang, Z., Xin, J., Yang, J., et al. 2022. "Synthesis and Characterization of Eu_2InTe_5: A New Layered Multitelluride and Its Thermoelectric Properties." *Physica Status Solidi (RRL)-Rapid Research Letters* 2022: 2200166.

[11] Kresse, G., and Furthmüller, J. 1996. "Efficiency of Ab-Initio Total Energy Calculations for Metals and Semiconductors Using a Plane-Wave Basis Set." *Comput. Mater. Sci.* 6: 15-50.

[12] Perdew, J. P., Burke, K., and Ernzerhof, M. 1996. "Generalized Gradient Approximation Made Simple." *Phys. Rev. Lett.* 77: 3865-8.

[13] Monkhorst, H. J., and Pack, J. D. 1976. "Special Points for Brillouin-Zone Interactions." *Phys. Rev. B* 13: 5188-92.

[14] Abbasi, A., and Khataee, A. 2019. "Band Gap Tunability and Structural Stability of Metal/Nonmetal Codoped Group-IV Tin Nanotubes: Effect of Spin-Orbit Coupling." *Physica E: Low-dimensional Systems and Nanostructures* 114: 113644.

[15] Ju, M. G., Dai, J., Ma, L., and Zeng, X. 2017. "Perovskite Chalcogenides with Optimal Bandgap and Desired Optical Absorption for Photovoltaic Devices." *Advanced Energy Materials* 7 (18): 1700216.

[16] Gajdoš, M., Hummer, K., Kresse, G., Furthmüller, J., and Bechstedt, F. 2006. "Linear Optical Properties in the Projector-Augmented Wave Methodology." *Phys. Rev. B* 73: 045112.

[17] Dadsetani, M., and Pourghazi, A. 2006. "Optical Properties of Strontium Monochalcogenides from First Principles." *Phys. Rev. B* 73: 195102.

[18] Shen, Y. Q., and Zhou, Z. X. 2008. "Structural, Electronic, and Optical Properties of Ferroelectric $KTa_{1/2}Nb_{1/2}O_3$ Solid Solutions." *J. Appl. Phys*. 103: 074113.